Structural Trends in Borrego Valley, California: Interpretations from SIR-A and SEASAT SAR

Patricia A. Schultejann
Geophysics Group, Los Alamos National Laboratory, Los Alamos, NM 87545

ABSTRACT: SIR-A and Seasat radar images of southern California are used to detect and define regional structural patterns in conjunction with detailed field studies. Northwest-trending features associated with the San Andreas fault system are dominant and are clearly depicted on the radar images. Recently mapped northeast-trending left-lateral faults of Cenozoic age are also well defined on the images. Several linear features detected by radar and not included on existing maps may be the traces of previously unrecognized major faults. A regional system of east-west-trending folds is revealed on the radar images and is the surface manifestation of Pleistocene to recent north-south compression in Borrego Valley. Evidence from the radar images suggests that related east-west-trending folds and faults continue into the margin of the Peninsular Ranges Batholith, and into the basement rock beneath the thick clastic wedge in Borrego Valley.

INTRODUCTION

THE UTILITY of airborne and satellite-based radar systems to detect and depict subtle geologic and structural features has been amply demonstrated by numerous studies spanning the last 25 years (Elachi *et al.*, 1982; Elachi, 1980; Sabins *et al.*, 1980; Schaber *et al.*, 1976; and others). The advent of the space shuttle program adds a new dimension to radar remote sensing with the deployment of the Shuttle Imaging Radar (SIR) series. Designed specifically to facilitate geologic analysis, these spaceborne synthetic aperture radar (SAR) systems promise to increase the versatility and applicability of radar to complement field studies in solving geologic problems.

Radar imagery, along with Landsat imagery, provides an important regional data set that complements detailed field mapping and photo-geology using color and black-and-white aerial photographs. Although useful in regional analysis, radar and Landsat imagery does not substitute for high-resolution images and field studies.

In this study, regional structural trends in radar imagery of Borrego Valley are investigated. Detailed ground mapping in many of the areas depicted by the radar images has already been completed by Engel and Schultejann (1984), Schultejann (1984), Sharp (1981), Sharp (1975), Sharp and Clark (1972), and Theodore and Sharp (1975). These studies include the use of both color and conventional black-and-white high resolution aerial photography, which provides an excellent data base for mapping and field observations. Many subtle but critical structures and geologic features, that are not detectable at radar wavelengths or resolutions, are easily discernible on aerial photographs. These include drag folds, detachment faults, and imbricate thrust complexes mapped by Engel and Schultejann (1984) and Schultejann (1984).

Unlike Landsat, which operates in the visible and near infrared portion of the spectrum, radar wavelengths are sensitive to surface roughness rather than composition. Lithologies are therefore inferred by the texture of the surface and differing erosional characteristics.

REGIONAL GEOLOGY

GEOLOGIC SETTING

Borrego Valley is part of the larger Imperial Valley and is located west of the Salton Sea along the eastern margin of the Peninsular Ranges Batholith in south-central California. Plutons of the eastern batholith are predominantly granodiorite and are mid-Late Cretaceous in age (Baird *et al.*, 1979; Silver *et al.*, 1979; Todd and Shaw, 1979; Larsen, 1948). The entire range has been uplifted ~5 to 12 km above the basement floor of the adjacent Salton Trough (Fuis *et al.*, 1982).

The broken and irregular boundaries of Borrego Valley are primarily the result of Late Cenozoic right-lateral motions along major strands of the San Jacinto fault zone. Reconstructions using formerly adjacent metasedimentary rocks of the Santa Rosa Cataclastic Zone reveal net slip of ~26 to 28 km (A. E. J. Engel, personal communication). Borrego Valley is bounded on the north by the Santa Rosa Mountains and on the south by strands of the Elsinore fault zone. Motion along this section of the Elsinore system appears to be primarily a dip-slip component (Schultejann, 1984; Lowman, 1980).

The floor of Borrego Valley is part of the down-

dropped blocks of the Salton Trough and is filled with a thick wedge of mid-Late Cenozoic clastic sediments and alluvium. A regional unconformity exists throughout the valley, characterized by Cenozoic sediments deposited upon Paleozoic metamorphic and Cretaceous crystalline rocks. The oldest exposed sediments in Borrego Valley are of Miocene age and are confined to the southeast margins of the valley (Woodard, 1974; Sharp, 1972; Dibblee, 1954).

The sedimentary section reveals a Neogene history in Borrego Valley of alternating marine and terrestrial deposition. The last marine transgression occurred in the Pliocene and resulted in deposition of the Imperial Formation (Woodard, 1974). Since then, terrestrial and lacustrine units have been deposited continuously up to the present (Dibblee, 1954).

STRUCTURAL FEATURES

The present topography of Borrego Valley is primarily a product of mid-Late Cretaceous plutonism and thrust faulting coupled with Cenozoic strike- and dip-slip faulting along strands of the San Andreas fault system, which includes the San Jacinto and Elsinore fault zones. These Late Cenozoic faults and batholithic blocks control the dominant northwest structural trend in Borrego Valley. Most of these northwest-trending faults are well known and documented; however, extensions of and motions along many of these strands are still unknown or equivocal (Johnson *et al.*, 1984; Lowman, 1984; Lowman, 1980; Crowell and Ramirez, 1979; Jennings, 1977; Merifield and Lamar, 1975; Sharp, 1972; Rogers, 1965).

Recent field mapping has revealed a second trend which consists of a number of left-lateral and left-oblique-slip faults. Most of these features occur in the marginal plutons that border Borrego Valley, and may represent a conjugate set of faults to the dominant right-lateral faults of the region. These faults are further discussed in Engel and Schultejann (1984) and Schultejann (1984).

Late Cretaceous folding and thrust faulting is well exposed along the eastern margin of the Peninsular Ranges Batholith in northern Borrego Valley, Clark Valley, and in the Santa Rosa Mountains (Engel and Schultejann, 1984). Metasedimentary rocks and marginal sections of batholithic plutons are thrust to the west over and to the north along the margin of the Peninsular Ranges Batholith. Associated folds range from microscopic to ~6 km in amplitude.

Mid-Cenozoic detachment faults are exposed along the batholithic margins of Borrego Valley from the Santa Rosa Mountains southward to Yaqui Ridge (Engle and Schultejann, 1984; Schultejann, 1984; Wallace and English, 1982). These faults slice through the marginal lobes of the batholith and extend the blocks along detachment surfaces or in a series of listric step faults. These step faults are best

exposed along the western edge of Borrego Valley and on eastern Coyote Mountain.

Folding in the Cenozoic sediments of Borrego Valley is known but has not been extensively researched (Sharp, 1972; Sharp and Clark, 1972; Dibblee, 1954). Detailed maps of the Ocotillo badlands are presented in Sharp and Clark (1972, Figures 92 and 93). These maps show a series of Pleistocene to present east-west-trending anticlines and synclines in the Cenozoic sedimentary section. The folds are intimately associated with strands of the San Jacinto fault zone, and appear to be a manifestation of transpressional tectonics (Sharp and Clark, 1972).

SIR-A AND SEASAT SAR DATA

Major system characteristics for SIR-A and Seasat SAR are summarized in Table 1. Two digitally correlated Seasat SAR scenes were used, each covering a portion of Borrego Valley and beyond. Because the images are extremely large (6144 by 6144 pixels), a subscene containing Borrego Valley was selected from each tape and digitally mosaicked to form a complete image of Borrego Valley (Figure 1).

The ability to observe structural features in a radar image depends on both depression angle and illumination direction. The steep depression angle of the Seasat SAR introduces a significant amount of "layover" distortion in high-relief terrain, but may enhance subtle topographic differences in relatively flat terrain. Layover is a geometrical displacement in the image, with the top of an object displaced toward the near range, relative to its base. Layover distortion is minimal in Borrego Valley itself, while the surrounding Peninsular Ranges are greatly affected. The look direction, or direction of propagation of the radar wave, for the Seasat image is to the ENE.

One swath was acquired by SIR-A over southern California. This image was optically correlated and black-and-white prints were made from photographic negatives. The major portion of Borrego Valley is included on a portion of this swath (Figure 2). Clark Valley, the Santa Rosa Mountains, and the extreme eastern edge of the San Felipe Hills were not acquired by SIR-A. Lay-over distortion is reduced on SIR-A images because of the moderate

TABLE 1.   SEASAT AND SIR-A RADAR PARAMETERS.*

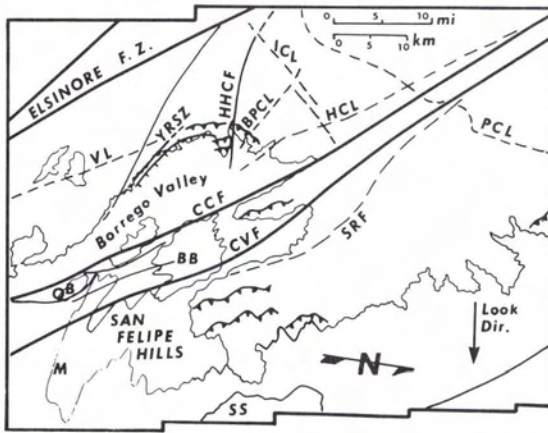|	Seasat	SIR-A
wavelength	23.5 cm (L-band)	23.5 cm (L-band)
frequency	1.275 GHz	1.278 GHz
resolution	25 m	40 m
incidence		
angle	23 ± 3°	50 ± 3°
swath width	100 km	50 km
polarization	HH	HH
signal		
correlation	Optical and digital	Optical

* From Ford *et al.* (1983).

FIG. 1. Seasat SAR mosaic and index map of Borrego Valley, California. Look direction is ENE, toward the bottom of the image. A = unmapped strands of the San Jacinto fault system along the Santa Rosa Mountains (SRF on index map); VL = Vallecito lineament; YRSZ = Yaqui Ridge shear zone; HHCF = Hell Hole Canyon fault; BPCL = Borrego Palm Canyon lineament; ICL = San Ysidro Creek fault (Indian Creek lineament); HCL = Henderson Canyon lineament; PCL = Palm Canyon lineament; CCF = Coyote Creek fault; CVF = Clark Valley fault; BB = Borrego Badlands; OB = Ocotillo Badlands; SS = Salton Sea.

depression angle. Look direction for the SIR-A image is to the northeast.

The factors which determine relative brightness in a radar image have been thoroughly discussed elsewhere and will not be covered in detail in this report (e.g., MacDonald (1980), Sabin (1978), and included reference lists). The primary surface parameters in an arid region are topography and surface roughness, while the major radar system factors are depression angle, look direction, and wavelength. Because the wavelengths of SIR-A and Seasat SAR are the same, the difference in image signatures of various geologic features is due primarily to dif-

ferences in depression angle, look direction, resolution, and differences produced by optical versus digital processing.

The radar roughness criteria, which determine whether a surface will appear smooth or rough to the incident radar beam and, hence, dark or bright on the image, are given for both SIR-A and Seasat in Table 2. For a further discussion of roughness criteria, see Sabins (1978), Schaber *et al.* (1976), and Peake and Oliver (1971).

RADAR IMAGE ANALYSIS

The northwest-trending faults of the Elsinore and San Jacinto fault zones are clearly depicted on both SIR-A and Seasat images (Figures 1 and 2). The Seasat image portrays probable strands of the well known San Jacinto zone that have not been mapped along the Santa Rosa Mountains (A on Figure 1). SIR-A images would most likely show the same pattern had they extended farther to the east.

The SIR-A images are superior to the Seasat in portraying extensions of these faults in the San Jacinto zone through the sediments and alluvium of Borrego Valley. Traces of the Coyote Creek fault, Superstition Mountain fault, and Clark Valley fault, which are not readily apparent on the ground, are clearly delineated on the SIR-A image (A on Figure 2, and see Figure 3). Differences between the radar's ability to detect these faults could be due to differences in depression angle, look direction, and/or environmental factors at time of image acquisition. (August 1978 acquisition for the Seasat SAR image; November 1981 for SIR-A image).

The left-lateral Hell Hole Canyon fault is well defined on both images. The Yaqui Ridge shear zone, however, cannot be easily detected on the Seasat image. The hummocky topography, which is characteristic of the shear zone, is too similar in slope orientation and surface roughness to be differentiated from surrounding terrain (Figure 1, and see Schultejann (1984)). The Yaqui Ridge shear zone is primarily in radar shadow on the SIR-A image because of the moderate depression angle of the SIR-A system.

Several prominent linear features are visible along the northwestern and southern margin of Borrego Valley and may represent major unmapped faults (Figures 1, 2, and 4). The Borrego Palm Canyon lineament, Vallecito lineament, and Henderson Canyon lineament trend northwest, parallel to the adjacent San Jacinto and Elsinore fault zones, and may be subsidiary strands to the major faults of those systems. The San Ysidro Creek fault (Indian Creek lineament) strikes northeast, sub-parallel to the left-lateral Hell Hole Canyon fault. The sense of motion on the San Ysidro Creek fault is unknown (Merifield and Lamar, 1975). The Salvador Canyon lineament is only apparent on the SIR-A image. This may be a result of layover interference in the Seasat SAR image or a more favorable orientation to look
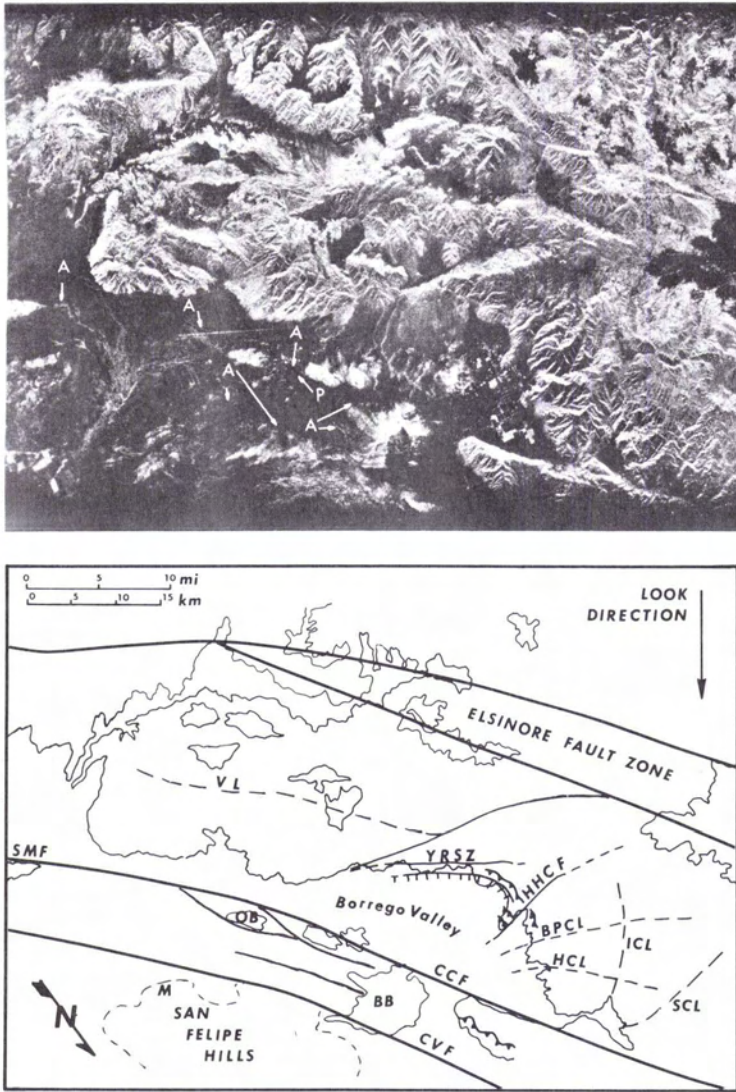
FIG. 2.   SIR-A image and index map of Borrego Valley, California. Look direction is NE, toward the bottom of the image. A = traces of the Coyote Creek fault, Superstition Mountain fault, and Clark Valley fault not easily identified from aerial photographs or on the ground; VL = Vallecito lineament; YRSZ = Yaqui Ridge shear zone; HHCF = Hell Hole Canyon fault; BPCL = Borrego Palm Canyon lineament; HCL = Henderson Canyon lineament; ICL = San Ysidro Creek fault (Indian Creek lineament); USCL = Salvador Canyon lineament; SMF = Superstition Mountain fault; OB = Ocotillo Badlands; CCF = Coyote Creek fault; BB = Borrego Badlands; CVF = Clark Valley fault.

direction on the SIR-A image. A major northeast-trending linear feature extends from the San Andreas fault south-westward to Lake Henshaw on the Elsinore fault zone. The lineament is subtly depicted on corresponding Landsat images. This feature is mapped as the Palm Canyon fault on its extreme northwest section, but no further extensions or hypothesized extensions have been noted (Rogers, 1965; Dibblee, 1954). Jennings (1977) maps this section as a thrust, but in the regional context this interpretation is equivocal. The Palm Canyon lineament crosses the San Jacinto fault zone with no

TABLE 2.   RADAR ROUGHNESS AND RAYLEIGH CRITERIA FOR SEASAT SAR AND SIR-A.

		Seasat	SIR-A
Rayleigh Criterion (from Simonett and Davis, 1983)	$h < \dfrac{\lambda}{8 \sin \theta}$	$h < \dfrac{23.5 \text{ cm}}{8 \sin 67°}$ $h < 3.2 \text{ cm}$	$h < \dfrac{23.5 \text{ cm}}{8 \sin 40°}$ $h < 4.6 \text{ cm}$
Smooth Criterion (from Peake and Oliver, 1971)	$h < \dfrac{\lambda}{25 \sin \theta}$	$h < \dfrac{23.5 \text{ cm}}{25 \sin 67°}$ $h < 1.0 \text{ cm}$	$h < \dfrac{23.5 \text{ cm}}{25 \sin 40°}$ $h < 1.5 \text{ cm}$
Rough Criterion (from Peake and Oliver, 1971)	$h > \dfrac{\lambda}{4.4 \sin \theta}$	$h > \dfrac{23.5 \text{ cm}}{4.4 \sin 67°}$ $h > 5.8 \text{ cm}$	$h > \dfrac{23.5 \text{ cm}}{4.4 \sin 40°}$ $h > 8.3 \text{ cm}$

where λ = wavelength,
θ = aspect angle (assuming a horizontal terrain surface), and
h = height of microrelief.

apparent offset, forms a semi-circular bend around a hemispherical outcrop of granodiorite, then continues southwestward into the Elsinore fault zone, where it is dragged into strands of this zone in a right-lateral pattern (Figure 4). The Palm Canyon structure appears to be a major rupture in the upper crust. Because it transects strands of the San Jacinto fault zone with little or no displacement, it deserves intensive field study.

The San Ysidro Creek fault and Palm Canyon lineament are readily discernible on Seasat images, but not well defined on the SIR-A image. The trend of both of these lineaments is parallel to the look direction of the SIR-A. This minimizes slope-induced brightness changes associated with the lineaments, and renders them nearly invisible on the SIR-A image. Features such as the San Jacinto fault zone, which are oriented perpendicular to the look direction, are enhanced on the radar images.

The zone of westward and northward imbricate thrust faults and folds cannot be detected on either SIR-A or Seasat SAR images. These zones are characterized by cataclastic rocks which weather in a similar pattern to the adjacent plutonic rocks, and the differences in surface roughness are too slight to be detected by the radar systems. Individual thrust faults are below the limit of resolution for either system, but can be easily identified on both color and black-and-white aerial photographs.

The mid-Cenozoic detachment faults are not well delineated on either image for the same reasons that the Yaqui Ridge shear zone is poorly depicted. The step faults along the margins of the valley, however, are clearly defined on both the SIR-A and Seasat SAR images. These faults are greatly distorted on the Seasat SAR image because of the layover effect in the mountainous terrain (Figure 1).

A conspicuous trend on both images is the banded pattern that extends throughout the valley from the western edge of the Salton Sea westward to the batholithic margin in northwestern Borrego Valley (Figures 1 and 2). The pattern indicates east-west-

FIG. 3.   Photograph of traces of the Coyote Creek fault NNW of the Ocotillo Badlands. Photo looks south from Borrego Mountain to the Ocotillo Badlands and corresponds to P on Figures 1 and 2. Lines indicate approximate trace of fault strands.
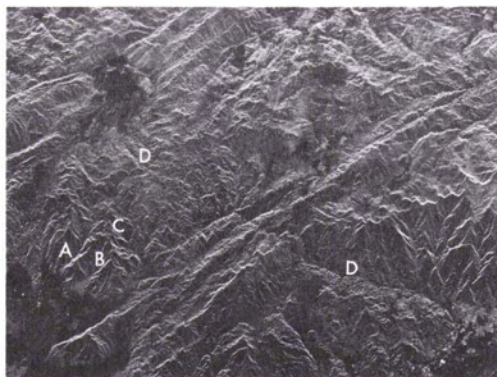
FIG. 4. Seasat SAR image of northwest Borrego Valley and Peninsular Ranges. Prominent linear features are *A* = Borrego Palm Canyon lineament; *B* = Henderson Canyon lineament; *C* = San Ysidro Creek fault; *D* = Palm Canyon lineament.
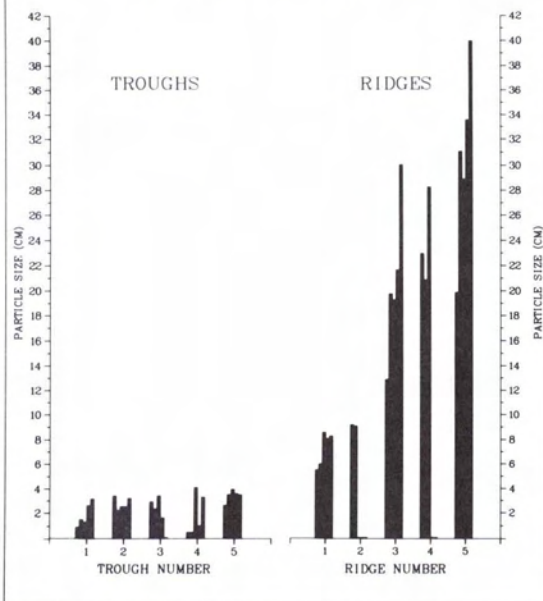

FIG. 6. Histogram of measurements taken from five ridges and troughs in the southern San Felipe Hills region. The largest particles were measured from 12 cells within a 1 m by 1 m sample area. Five sample areas were taken, 150 m apart, along the axis of each of the five ridges and troughs. The bimodal distribution shows a significant difference in size of largest particles for ridges and troughs.

trending strips of ground surface that are alternately smooth and rough at the 23.5 cm radar wavelength. The extreme southeastern portion of the region coincides with Pleistocene folds mapped by the Sharp and Clark in the Ocotillo badlands (Sharp and Clark (1972), Figures 92 and 93). Field studies in the region reveal a series of east-west-trending anticlines and synclines in the Plio-Pleistocene sediments (Figure 5). A ridge is produced where erosionally resistant sandstone and sandy shale beds are preferentially preserved relative to the more easily eroded silts and muds of intervening units (Figure 5).

The microrelief was measured on five ridges and troughs along the southern edge of the San Felipe Hills (M on Figures 1 and 2). Five areas, 150 m apart, were sampled along the axis of each ridge and trough. Each sample area measured 1 m by 1 m and was divided into a grid containing 12 cells. Each

FIG. 5. Photograph of anticlines and synclines in Plio-Pleistocene sediments in the San Felipe Hills region of Borrego Valley. Ridges and troughs were sampled for microrelief and the area is indicated by *M* in Figures 1 and 2.

cell was sampled and the largest particle in the cell recorded. Where constituent particles measured less than 0.5 cm or greater than 30 cm, the measurements were not recorded.

Microrelief on the sampled ridges is significantly higher than microrelief on the sampled troughs, with ridge averages varying from 5.5 cm to >40 cm (Figure 6 and Table 3). In all but one case, the average microrelief exceeds the rough criterion and Rayleigh criterion for both Seasat SAR and SIR-A (Tables 2 and 3).

Two of the sampled ridges (No. 2 and No. 4) are composed partially of fine silt and sand particles (<0.1 cm). However, the erosional pattern displayed by these ridges is a series of facets and gullies which produce a strong backscatter component and resultant bright image signature (Figure 7).

The intervening troughs are very flat and covered with mud, sand, and pea gravel ranging from <0.1 cm to 3.4 cm (Figure 6 and Table 3). Most of the microrelief averages for the sample site are below the Rayleigh criterion. However, most of the average measurements slightly exceed the criterion derived by Peake and Oliver (1971) for smooth surfaces (Table 2 and Figure 6). The controlling factor

TABLE 3. MEAN AND STANDARD DEVIATION OF SURFACE ROUGHNESS (MICRORELIEF) FROM FIVE RIDGES AND TROUGHS IN THE SOUTHERN SAN FELIPE HILLS REGION.

5 sample sites/ridge or trough
$n = 12$/sample site

Trough Sample Site		Trough 1	Trough 2	Trough 3	Trough 4	Trough 5
(1)	$\bar{x}$(cm)	0.9	3.4	2.9	sand < 0.5	2.6
	s	0.3	0.6	0.5		0.8
(2)	$\bar{x}$(cm)	1.5	2.2	2.3	sand < 0.5	3.5
	s	0.5	0.7	0.6		0.7
(3)	$\bar{x}$(cm)	1.3	2.5	3.3	4.0	3.0
	s	0.3	0.8	0.8	1.2	0.6
(4)	$\bar{x}$(cm)	2.6	2.5	1.7	sand < 1.0	3.6
	s	1.5	0.5	0.4		1.0
(5)	$\bar{x}$(cm)	3.5	3.3	flat muds	3.3	3.5
	s	1.4	0.7		1.0	1.0

Ridge Sample Site		Ridge 1	Ridge 2	Ridge 3	Ridge 4	Ridge 5
(1)	$\bar{x}$(cm)	5.5	9.2	12.1	23.0	19.9
	s	1.5	2.8	3.4	5.5	1.6
(2)	$\bar{x}$(cm)	6.0	9.1	19.8	20.9	31.0
	s	2.0	1.3	2.2	5.9	2.6
(3)	$\bar{x}$(cm)	8.6	badland	19.3	28.3	28.9
	s	3.0	(see Figure 7)	5.9	8.4	2.7
(4)	$\bar{x}$(cm)	8.0	badland	21.7	badland	33.6
	s	1.0		4.9		3.0
(5)	$\bar{x}$(cm)	8.3	badland	sandstone slabs > 30.0	badland	sandstone slabs > 30.0
	s	1.7				

appears to be the density of larger particles on the target surface (Figure 8). Although the troughs contain particles larger than the size specified for the smooth criterion, the particles appear to be small enough, and the densities low enough, so that the average roughness per resolution cell is below the criterion.

These ridges and troughs are the surface manifestation of east-west oriented axes of anticlines and synclines which occur throughout the valley. The spacing of the bands is an indication of the wavelength of the folds. Where the sediments are tightly folded, specific lithologic sections are repeated many times and many bands appear on the images. Conversely, where folds are gentle, lithologic sections repeat infrequently, and broad widely-spaced bands result. This can clearly be seen in the Borrego Badlands, which consists of one large synclinorium (Dibblee (1954) and Figures 1 and 2). Throughout the synclinorium the topography is badland, without the flat, pebble-covered drainage troughs. The facets and corners that are characteristic of badland formations create relatively strong radar return, and the region has a uniformly bright radar signature.

The radar images indicate that the east-west structural grain is of regional extent, a point previously unrecognized from detailed ground studies. The east-west structures are present in the surrounding batholithic rocks in addition to Borrego Valley. The Yaqui Ridge antiform, San Felipe fault,
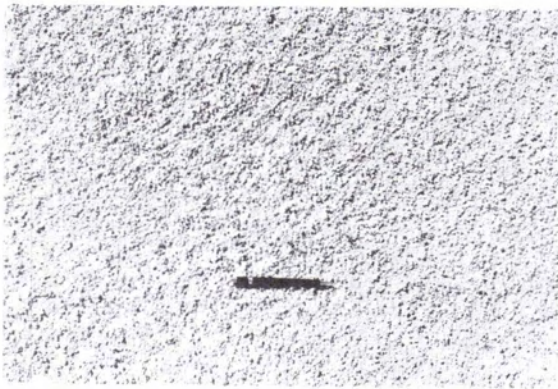

FIG. 7. An example of "badland" topography from ridge No. 2. Erosion of siltstones and mudstones which compose the ridge results in a series of facets and gullies which produce a strong backscatter component. Constituent particles average <0.1 cm.

High Density
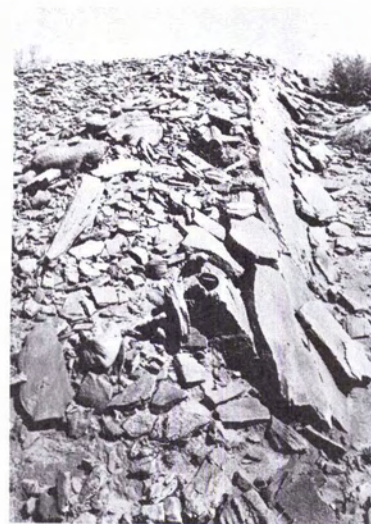
High Density

Low Density

Low Density

FIG. 8.   Photographs showing the relative densities of larger particles on ridges (right) and troughs (left) in the southern San Felipe Hills. Size and densities of large particles in the troughs are low enough so that the average microrelief in a single resolution cell is below the smooth criterion, and a dark radar signature results.

Yaqui Ridge shear zone, and Hell Hole Canyon fault are all roughly aligned with this trend. Remnants of east-west-trending folds in Plio-Pleistocene sediments can be detected as far north as Clark Lake playa and as far south as the southwestern edge of Borrego Valley, south of Borrego Springs (Engel and Schultejann, 1984).

It seems likely that the east-west structural trend also extends into the basement of Borrego Valley. Groundwater studies in Borrego Valley have revealed an east-west-trending drainage divide which inhibits the flow of ground water from the northern section of the valley to the south (Burzell and Treet, 1979). Additionally, trilateration surveys along the major faults in southern California have measured uniaxial north-south compression of ~0.2 to 0.3 strain/yr (Savage et al., 1979; 1978). It is probable that the east-west trending folds and faults are surface manifestations of that strain and continue to some depth into the basement of Borrego Valley.

There are two areas in Borrego Valley where the east-west trend has been somewhat distorted. The first of these is a small section of folds in southwestern Borrego Valley, just north of Yaqui Ridge (Figures 1 and 2). The axes of the folds in this area strike east-northeast, about 20° counter-clockwise from the axes of other folds in the valley. This section is bounded on the north by strands of the Coyote Creek fault. However, there is no apparent bounding fault along the southern edge.

The second region lies adjacent to the Santa Rosa Mountains and comprises the northern section of the San Felipe Hills. Here, the axes of the folds trend east-west in the eastern portion of this area (Figure 1). However, as the folds approach the Santa Rosa fault, they attain a more northwesterly orientation. This phenomenon may be produced by one or a combination of two mechanisms: (1) The uplift of the Santa Rosa Mountains may be a "trapdoor" variety, with metasediments and sediments dipping

to the east (Figure 11 of Engel and Schultejann (1984)); thus, the sediments on the western margin are displaced and elevated to a greater degree relative to the sediments on the eastern margin, causing an apparent northward bend; and (2) the change in orientation of the axes of the folds reflects actual right-lateral drag along the Santa Rosa fault.

CONCLUSIONS

SIR-A and Seasat SAR images have proven useful in the regional structural analysis of Borrego Valley and can be used to complement field studies and air-photo analysis at relatively higher resolutions. This imagery has proven valuable in the determination of regional fault and joint patterns, to allow extension of the traces of unknown faults, and to delineate regional fold patterns not readily apparent from air photos and field studies.

A regional east-west alignment of Plio-Pleistocene fold axes and faults is revealed on both SIR-A and Seasat radar images. These features are expressed on the images as a series of alternating bands of bright and dark radar signatures that correspond to ridges and troughs of anticlines and synclines in Cenozoic clastic sediments. The folds are the surface manifestation of a fairly young north-south compressive strain that continues to the present in Borrego Valley. The east-west-trending folds continue into the margin of the batholith and presumably into basement rocks beneath the sedimentary fill of Borrego Valley.

ACKNOWLEDGMENTS

Many thanks to Tim Dixon and Jet Propulsion Laboratory for providing images and tapes, U.S. Geological Survey in Flagstaff for images and support, and Zonta International for the Amelia Earhart Fellowship. I also wish to thank the three reviewers and Dr. Al Engel for their helpful comments and advice.

REFERENCES

Baird, A. K., K. W. Baird, and E. E. Welday, 1979. Batholithic rocks of the northern Peninsular and Transverse Ranges, southern California: Chemical composition and variation, in *Mesozoic Crystalline Rocks, Peninsular Ranges Batholith and Pegmatites, Point Sal Ophiolite*, P. L. Abbott and V. R. Todd, eds., Guidebook for GSA Annual Meeting, San Diego, California, pp. 177-231.

Burzell, L. R., and R. L. Treet, 1979. *Hydrology Report for Environmental Impact Report, Ram's Hill Five Year Plan*, 11 p.

Crowell, J. C., and V. R. Ramirez, 1979. Late Cenozoic faults in southeastern California, in *Tectonics of the Juncture between the San Andreas Fault System and the Salton Trough, Southeastern California*, J. C. Crowell and A. G. Sylvester, eds., Santa Barbara, Univ. of Calif., Dept. of Geology, 193 p.

Dibblee, T. W., Jr., 1954. Geology of the Imperial Valley Region, California, in *Geology of Southern California*, R. H. Jahns, ed., California Div. Mines Bull, 170, Chap. 2, pp. 22-28.

Elachi, C., 1980. Spaceborne imaging radar: Geologic and oceanographic applications, *Science*, 209, pp. 1073-1082.

Elachi, C., W. E. Brown, J. B. Cimino, T. Dixon, D. L. Evans, J. P. Ford, R. S. Saunders, C. Breed, H. Masursky, J. F. McCauley, G. G. Schaber, L. Dellwig, A. England, H. MacDonald, P. Martin-Kaye, and F. Sabins, 1982. Shuttle imaging radar experiment, *Science*, 218, pp. 996-1003.

Engel, A. E. J., and P. A. Schultejann, 1984. Late Mesozoic and Cenozoic tectonic history of southcentral California, *Tectonics*, 3, pp. 659-675.

Ford, J. P., J. B. Cimino, and C. Elachi, 1983. *Space shuttle Columbia views the world with imaging radar: the SIR-A experiment*, JPL publication 82-95, 179 p.

Fuis, G. S., W. D. Mooney, J. H. Healy, G. A. McMechan, and W. J. Lutter, 1982. Crustal structure of the Imperial Valley region, in *The Imperial Valley, California, Earthquake of October 15, 1979*, U.S.G.S. Prof. Paper 1254, pp. 24-49.

Jennings, C., 1977. *Geologic Map of California, 1:750,000*, Calif. Div. Mines and Geology.

Johnson, N. M., C. B. Officer, N. D. Opdyke, G. D. Woodward, P. K. Zeitler, and E. H. Lindsay, 1984. Comment and Reply on "Rates of late Cenozoic tectonism in the Vallecito-Fish Creek basin, western Imperial Valley, California," *Geology*, 12, p. 320.

Larsen, E. S., Jr., 1948. *Batholith and Associated Rocks of Corona, Elsinore and San Luis Rey Quadrangles, Southern California*, Geol. Soc. Am. Memoir 29, 182 p.

Lowman, P. D., Jr., 1980. Vertical displacement on the Elsinore fault of southern California: Evidence from orbital photographs, *J. Geology*, 88, pp. 415-432.

———, 1984. Comment and Reply on "Rates of late Cenozoic tectonism in the Vallecito-Fish Creek basin, western Imperial Valley, California," *Geology*, 12, p. 319.

MacDonald, H. C., 1980. Techniques and applications of imaging radars, in *Remote Sensing in Geology*, B. S. Siegal and A. K. Gillespie, eds., John Wiley and Sons, Chap. 10, pp. 297-336.

Merifield, P. M., and D. L. Lamar, 1975. Active and inactive faults in southern California viewed from Skylab, *Proceedings of the NASA Earth Resources Symposium*, 1-B, pp. 779-797.

Peake, W. H., and T. L. Oliver, 1971. *The response of terrestrial surfaces at microwave frequencies*, Ohio State Univ. Electrosci. Lab 2440-7, Technical Report AFAL-TR-70-301, 255 p.

Rogers, T. H., (compiler) 1965. *Geologic Map of California, Santa Ana Sheet*, 1:250000.

Sabins, F. F., 1978. *Remote Sensing: Principals and Interpretation*, W. H. Freeman and Co., San Francisco, 426 p.

Sabins, F. F., R. Blom, and C. Elachi, 1980. Seasat radar image of the San Andreas fault, California, *Am. Assoc. Petrol. Geol. Bull*, 64, pp. 619-628.

Savage, J. C., W. H. Prescott, M. Lisowski, and N. King, 1978. Strain in southern California: Measured uniaxial

north-south regional contraction, *Science*, 202, pp. 883-885.

———, 1979. Deformation across the Salton Trough, California, 1973-1977, *J. Geophys. Research*, 84, pp. 3069-3079.

Schaber, G. G., G. L. Berlin, and W. E. Brown, 1976. Variations in surface roughness in Death Valley, California-Geologic evaluation of 25-cm wavelength radar images, *Geol. Soc. Am. Bull.*, 87, pp. 24-41.

Schultejann, P. A., 1984. The Yagui Ridge antiform and detachment fault: Mid-Cenozoic extensional terrane west of the San Andreas fault, *Tectonics*, 3, pp. 677-691.

Sharp, R. V., 1972. Tectonic setting in the Salton Trough, in *The Borrego Mountain Earthquake of April 9, 1969*, U.S. Geol. Survey Prof. Paper 787, pp. 3-15.

———, 1975. En echelon fault patterns of the San Jacinto fault zone, in *San Andreas Fault in Southern California*, J. C. Crowell, ed., Calif. Div. Mines and Geol., pp. 147-152.

Sharp, R. V., and M. M. Clark, 1972. Geologic evidence of previous faulting near the 1968 rupture on the Coyote Creek faults, in *The Borrego Mountain Earthquake of April 9, 1968*, U.S. Geol. Surv. Prof. Paper 787, pp. 131-140.

Silver, L. T., H. P. Taylor, and B. Chappel, 1979. Some petrological geochemical, and geochronological observations of the Peninsular Ranges Batholith near the international border of the United States of America and Mexico, in *Mesozoic Crystalline Rocks: Peninsular Ranges Batholith and Pegmatites, Point Sal Ophiolite*, P. L. Abbott and V. R. Todd, eds., Guidebook for the GSA Annual Meeting, San Diego, California, pp. 83-110.

Theodore, T. G., and R. V. Sharp, 1975. *Geologic map of the Clark Lake quadrangle, San Diego County, California*, U.S. Geol. Survey Map MF-644.

Todd, V. R., and S. E. Shaw, 1979. Structural, metamorphic, and intrusive framework of the Peninsular Ranges Batholith in southern San Diego County, California, in *Mesozoic Crystalline Rocks: Peninsular Ranges Batholith and pegmatites, Point Sal Ophiolite*, P. L. Abbot and V. R. Todd, eds., Guidebook for the GSA Annual Meeting, San Diego, California, pp. 177-231.

Wallace, R. D., and D. J. English, 1982. Evaluation of possible detachment faulting west of the San Andreas, southern Santa Rosa Mountains, California, in *Mesozoic-Cenozoic Tectonic Evolution of the Colorado River Region, California, Arizona, and Nevada*, E. G. Frost and D. L. Martin, eds., Geol. Soc. Am. Anderson-Hamilton Volume, pp. 502-509.

Woodard, G. D., 1974. Redefinition of the Cenozoic stratigraphic column in Split Mountain Gorge, Imperial Valley, California, *Am. Assoc. Petro. Geol. Bull.*, 58, pp. 521-525.

Remote Sensing In Anthropology and Archaeology

Washington Hilton, Washington, D.C.
6-7 December 1985

Among topics to be addressed at this day-long symposium—being held during the annual meeting of the American Anthropology Association—are ethical questions concerning the use of remote sensing in anthropology (especially third world contexts), future technologies and directions of research, and the proposed commercialization of Landsat and the effects of other policy decisions on research. Participants in the symposium are many of the more active researchers in remote sensing, and an ample discussion period has been allowed so that they and members of the audience might interact. Those who are already knowledgeable and those who would like to become knowledgeable about how remote sensing technology is being integrated into anthropological and archaeological research designs are cordially invited to attend.

Persons interested in being included on the mailing list of a proposed *Remote Sensing Newsletter*, the first number of which will be a report on the symposium, should contact

Scott Madry
Department of Anthropology
University of North Carolina
Chapel Hill, NC 27514